PROCEEDINGS, 49th Workshop on Geothermal Reservoir Engineering
Stanford University, Stanford, California, February 12-14, 2024
SGP-TR-227

An Efficient Annual-Performance Model of a Geothermal Network for Improved System Design, Operation, and Control

Juliet G. Simpson and Guangdong Zhu

National Renewable Energy Laboratory, Golden, CO 80401

Juliet.Simpson@nrel.gov

Keywords: geothermal network, district heating and cooling, district energy system, heat pump, geothermal heat pump, ground-source heat pump, borehole, control, thermal energy network, ambient-temperature loop

ABSTRACT

Geothermal district energy systems (DES), and specifically geothermal networks, provide a viable solution for decarbonizing residential and commercial heating and cooling loads. District energy systems of all kinds enable a thermal resource with a relatively high capital cost (such as a geothermal borehole field) to be shared among a large number of users. While district heating and cooling has been studied for many years, geothermal networks, fifth generation DES that utilize water-source heat pumps and an ambient temperature loop to meet heating and cooling loads, have not been implemented extensively and thus require additional technical and economic optimization to obtain maximum benefits.

This paper presents a newly developed reduced-order model that captures the flow of energy within the network, including the commercial and residential users' electrical usage, at an hourly rate over a year. The model includes building loads, heat pumps, borehole fields, and auxiliary heat/cool input, all connected with an ambient-temperature thermal loop model. In the model, operational control is possible for the borehole fields, circulation pump, and auxiliary system. For a given system, the model can output the complete state parameters for each component, the thermal loop, and the collective system, such as flow rate over time, average thermal loop temperature over time, and total electricity usage. The model can also be used to optimize the system control for maximizing system efficiency or minimizing system operational cost. For example, one initial assessment of the borehole controller for an example system showed that a controller with on/off operation of the borehole field reduces annual electrical usage by 33%, compared with continuous operation mode. Hence, the model can assist in optimizing a given system's operation to get the most value out of a geothermal network installation. Future work will consider the model's application to a demonstration project, including the model validation against operational data and system operation optimization.

1. INTRODUCTION

District energy systems (DES) that utilize water-source heat pumps are an important method for reducing carbon production from heating and cooling loads. Buffa (2019) defines a fifth generation (5G) network as a thermal energy network whose temperature is not suitable for direct heating and instead requires the use of a water-source heat pump to provide heating. A 5G DES includes an ambient-temperature loop (more generally called a thermal loop or thermal network) which connects buildings in a district or network to each other and any load balancing sources such as boreholes, solar thermal, or wastewater heat exchange. Buildings interface with the thermal loop via individual water-source heat pumps which are then able to meet the individual building heating and cooling loads. Uniquely, an ambient-temperature loop does not have pipe insulation and thus does not attempt to keep the working fluid temperature significantly different from the ground temperature. Instead, the loop temperature stays near the ground temperature (at around 5 ft deep) though it may vary both seasonally and based on the heat exchanged with building loads and different thermal sources. Herein, we refer to a 5G DES with a single-pipe ambient-temperature loop that utilizes geothermal energy as a geothermal network.

Not only do heat pumps eliminate the on-site use of fossil fuels, heat pumps are more efficient at converting energy into heat than direct fossil fuel heating. Geothermal or ground-source heat pumps (GHP or GSHP) perform better than air-source heat pumps in most locations because GHPs exchange heat at near-constant temperatures with the shallow subsurface, rather than exchanging heat with variable ambient air temperature. The national GHP study performed by Liu et al. (2023) found significant benefits from converting individual existing building heating and cooling systems to geothermal heat pumps, including reduced power costs for all grid users and a net reduction in annual electricity consumption.

A networked system of heat pumps (like a geothermal network) is expected to result in even more significant benefits to the electrical grid because thermal inertia can smooth demand peaks. Additionally, connecting heat pumps with an ambient-temperature loop rather than using individual geothermal heat pumps results in shared capital cost which can result in more equitable deployment.

Ambient-temperature loops also allow for the bi-directional flow of energy, where buildings in the district can both consume heat from the system and produce heat for the system (Buffa et al., 2019). These users are called "prosumers". The mix of heating and cooling loads on the thermal loop may result in "thermal load cancelling" where heat is moved from one user to another and the thermal loop temperature does not change significantly. When heating and cooling loads do not balance each other, a central plant or auxiliary system may be needed to help balance the system and maintain the thermal loop temperature within acceptable operating limits (Zarin Pass et al., 2018).

Small temporal mismatches in heating and cooling loads may be smoothed by thermal inertia in the system and may not need extra balancing load.

The thermal loop temperature may vary due to building loads, ground temperatures, and load balancing resources, but the ambient-temperature loop temperature tends to fall between 5-25°C (Buffa et al., 2019). Due to the low temperature of the working fluid in the system, higher flow rates are required to supply sufficient heat exchange to meet thermal demand and thus 5G systems require larger pipes and pumps (Sommer et al., 2020). Control of the thermal loop flow rate is one opportunity for improving performance and reducing parasitic loads (such as pumping power) while utilizing the same system equipment.

The major components to capture in a 5G DES model include the ambient-temperature loop (including thermal inertia and thermal transport), heat exchange with building heat pumps, heat exchange with boreholes (or other balancing sources), circulation pump flow rate, and electricity inputs. For in-depth design of DES, TRNSYS (commercial) or Modelica-based (open-source) models are often used. The Modelica Buildings Library (Lawrence Berkeley National Laboratory, n.d.) is the basis for many Modelica-based models. However, these options are complicated, computationally expensive, and (in the case of TRNSYS) not publicly available. Additional models have been created by researchers to fill specific needs for modeling different systems or subcomponents (including Refs.(del Hoyo Arce et al., 2018; Quirosa et al., 2022)), such as capturing more complex fluid dynamics in the thermal loop. There still exists a need for a publicly available, fast, reduced-order model that can capture the critical aspects of a DES for system design and analysis.

While the components of a geothermal network are well established, the combined application has only been implemented in a few cases. Most notably, Colorado Mesa University has been operating a geothermal network since 2008 and has seen significant benefits including a 75% reduction in fossil fuel emissions from heating and cooling (EPRI, 2021; Xcel Energy, 2023). In addition to Colorado Mesa University, a geothermal network has been installed in the Whisper Valley housing development in Texas, showing the applicability of 5G systems in a residential environment (Marin, 2022; Oh & Beckers, 2023; Wolfson & Mapel, 2020).

A geothermal network has not yet been implemented in a suburban, retrofitted (brownfield) location in the United States. The Learning from the Ground Up (LeGUp) project[1] in Massachusetts is studying the first utility-led installations of these networked systems. Specifically, these installations are geothermal networks, so they will include an ambient-temperature single pipe network connecting buildings, ground-source heat pumps at each building, and one or more borehole fields. The goal of this paper is to create a generalized reduced-order model for simulating the performance and control of such geothermal networks that can later be used to model and assess the performance of the utility installations.

2. MODEL DESCRIPTION

A reduced-order model was written in Python to capture the flow of energy around the network and the electricity usage of the system over time. The reduced-order model uses simple representations of model components to capture the important behavior of the system with minimal computational time. The model will be posted publicly to GitHub upon validation with field test data and is available now upon request. The core of the model is the thermal loop and the central station (including the circulation pump), with the option for placement of modular components around the thermal loop: borehole fields, buildings with heat pumps, and auxiliary heating and cooling. The thermal loop is at “ambient temperature” which means that the temperature may vary but will remain near the temperature of the ground. Because the thermal loop does not directly provide heating or cooling, the temperature does not have to fall within as strict temperature limits as more traditional (3G) district heating and cooling systems. An overview of the major components in the model is shown in Fig. 1, where each of the modular components may be repeated many times around the thermal loop. Minor components such as piping and valves are not included in Fig. 1 but are generally included in the model.

[1] https://www.heet.org/legup

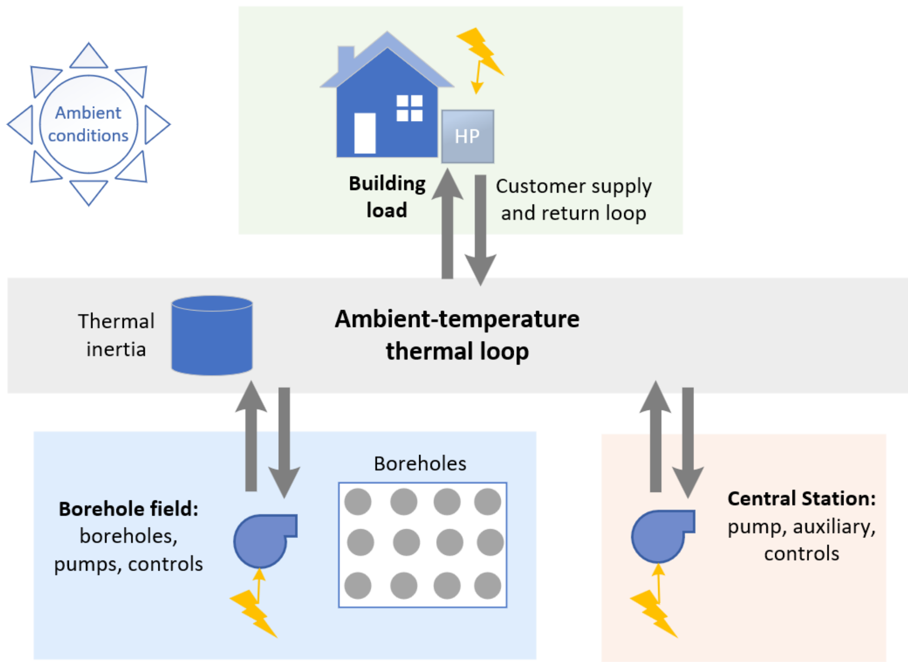

Figure 1. Reduced-order model components overview including ambient temperature loop, buildings, borehole fields, and central station.

2.1 Component models

The working fluid in the thermal loop is modeled herein as a mixture of water and propylene glycol (antifreeze solution). The mixture's glycol percentage can be varied from 0-60% within the model. Though around 20% glycol is common, systems can also be designed without any antifreeze solution in the working fluid, as demonstrated at Colorado Mesa University. The properties of the mixture are calculated based on temperature using SecondaryCoolantProps (Mitchell & Lee, 2022) and the fluid is assumed to be incompressible in the system. The modeling of thermal inertia of the working fluid is discussed in Section 2.2. The full thermal loop circulation pump power is calculated to overcome frictional losses and maintain the set flow rate.

Building loads are simulated using reference building models in URBANopt (Kontar et al., 2020), which runs OpenStudio/EnergyPlus simulations and outputs heating and cooling loads for each building in the district at the specified time-step interval (herein, hourly). A local TMY3 weather file was used for the building loads simulations. Building thermal loads are met with a water-source heat pump connected to the thermal fluid loop. The heat pump performance is estimated via a look-up table for heating and cooling coefficients of performance (COPs) based on thermal loop temperature, using data from ClimateMaster Tranquility TED/H/V 038 water-source heat pump (Climatemaster, 2022). The resultant electrical load is calculated. The effect of partial loading on the heat pumps is not considered. If building load or heat pump load timeseries data is available for users, then that data should be substituted for the simulated loads.

The borehole field performance is also assessed based on a look-up table. The data for the table was generated by a collaborator (Jianjun Hu, 12/11/2023) based a sweep of G-function simulation runs in Modelica with different ground temperatures, mass flow rates, and thermal loop temperatures. The look-up table estimates the temperature of the working fluid leaving the borehole field based on the temperature of the fluid entering the field and the mass flow rate. The change in ground temperature due to heat transfer is also tracked over time and if a significant change is seen, then the look-up table can be adjusted accordingly. Pumping power to operate the borehole fields and overcome the frictional losses is also calculated as described in Eqs. 1-5 below.

The auxiliary system is currently assumed to operate with a COP of 1 (representative of electric resistive heating), though depending on the system needs, auxiliary heating or cooling could be provided by natural gas, air-source heat pumps, or cooling towers. Ideally the auxiliary system would not be needed, and as such, the auxiliary system component is mostly used to track if any external heat transfer is needed to maintain the thermal loop temperature within acceptable bounds.

We have assumed that no heat transfer occurs between the thermal loop distribution pipe and the ground (heat transfer to the ground occurs only at the borehole fields), because the heat transfer at the borehole fields is assumed to be much more significant. However, depending on the buried depth of the thermal loop and temperature difference between the thermal loop and ground, the heat transfer between the thermal loop and the ground may be important and should be investigated in the future.

2.2 Thermal-fluid model

Once the performance of the major components is modeled with the reduced-order models, capturing the movement of heat and mass around the thermal loop piping is key. While the thermal loop pipe is not physically insulated, we have assumed that it is adiabatic between components and thus heat transfer only occurs when the thermal loop interacts with the major thermal components. The working fluid in the thermal loop acts as short-term storage and has thermal inertia that buffers loads that are put into the system. Thus, a large influx of heat at one point on the thermal loop will take a finite amount of time to reach and affect other parts of the thermal loop.

Simulation results for the district are recorded on an hourly basis. While analyzing loads on an hourly basis is common practice, we recognize that this may smooth over and miss shorter duration electricity peaks. For each hour, heating and cooling loads are prescribed based on building simulations and are assumed to be constant for the duration of the hour. The hydraulic model operates as a steady-state model for each hour; thus, the flow rate in the thermal loop has a one-hour operational timestep and pressure calculations are performed assuming steady conditions with viscous losses. The viscous losses in the thermal loop are calculated as follows using the Colebrook equation (Bergman et al., 2011).

$$u = \frac{\dot{m}}{\rho * \frac{\pi}{4} D^2} \tag{1}$$

$$Re = \frac{\rho u D}{\mu} \tag{2}$$

$$\frac{1}{\sqrt{f}} = -2 \log \left[\frac{\frac{\epsilon}{D}}{3.7} + \frac{2.51}{Re\sqrt{f}} \right] \tag{3}$$

$$P_{loss} = f \frac{L}{D} \frac{1}{2} \rho u^2 \tag{4}$$

where u is the flow speed, $\dot{m}$ is the mass flow rate of the working fluid in the thermal loop, ρ is the density of the working fluid, D is the thermal loop pipe inner diameter, μ is the working fluid viscosity, ϵ is the pipe roughness, f is the friction factor, and L is the length of the thermal loop. The viscous losses in the boreholes are calculated using the same equations. The resultant pumping power used to run the circulation pump and the borehole pumps is thus calculated as

$$W = P_{loss} \frac{\dot{m}}{\rho \eta} \tag{5}$$

where η is the pump efficiency, assumed to be constant at 70%. Note that while most valves on the thermal loop are accounted for with additional minor losses, some minor losses in the hydraulic system from redundancy valves or pipe constrictions or expansions are not included.

The thermal model is transient within each hour and operates on smaller timesteps—on the order of one minute. Rather than capturing the movement of heat and mass around the thermal loop with a fine mesh, the thermal loop is subdivided into equal-sized sections, each of which acts as a node or reservoir. The more sections, the more precise the temperature measurements can be, but the longer it takes to simulate. The thermal loop fluid in each section is assumed to be isothermal and isobaric. The working fluid then moves directly from one discrete node to the next. Heat is assumed to only propagate through the thermal loop via the flow of the working fluid. There is assumed to be no conduction of heat within the thermal loop from node to node; thus, heat cannot move against the direction of flow in the thermal loop. The small timestep size (dt) is chosen for each hour based on the thermal loop flow rate, such that the total section fluid moves from one section to the next in the small timestep,

$$dt = \frac{dx}{u} \tag{6}$$

where dx is the section length and u is the thermal loop speed in the given hour.

At each small timestep, heat is exchanged with any elements within that section (such as buildings, borehole fields, or auxiliary systems). The total heat exchanged with the section (Q_{HX}) during the small timestep from external sources is calculated as

$$Q_{HX} = (\dot{Q}_{buildings} + \dot{Q}_{boreholes} + \dot{Q}_{aux})dt \tag{7}$$

where $\dot{Q}_{buildings}$ is the heat rate transferred from building heat pumps, $\dot{Q}_{boreholes}$ is the heat rate transferred from borehole fields, and $\dot{Q}_{boreholes}$ is the heat rate transferred from the auxiliary system.

The fluid mass in the section is equal to the mass transferred during the time period because the timestep dt is sized such that the working fluid moves one section length for every time period. Thus, the mass of the section and the mass transferred is calculated as

$$m = \rho \frac{\pi}{4} D^2 dx \tag{8}$$

The starting temperature in the section (T_0), final temperature in the section (T_1), incoming fluid temperature (T_{in}), and outgoing fluid temperature (T_{out}) are all tracked. Herein we assume that the outgoing thermal loop temperature is equal to the final section temperature, $T_{out} = T_1$.

The heat transferred into the section from mass flow (Q_{mass}) is calculated as

$$Q_{mass} = mC_p(T_{in} - T_{out}) \tag{9}$$

where C_p is the specific heat of the working fluid as a function of temperature.

The new temperature of that section (T_1) is calculated at the end of each timestep based on the energy balance of heat and mass flows in and out and the thermal mass currently in the section. The energy balance for the section is written as follows

$$Q_{HX} + Q_{mass} = mC_p(T_1 - T_0) \tag{10}$$

While this section method loses some granularity of the temperature flow (depending on the number of sections), it allows for fast simulations that still capture the thermal inertia of the thermal loop.

At the end of each hour, results from the smaller timesteps are compiled back to the larger timestep size and saved. An overview of the code process is shown in Fig. 2.

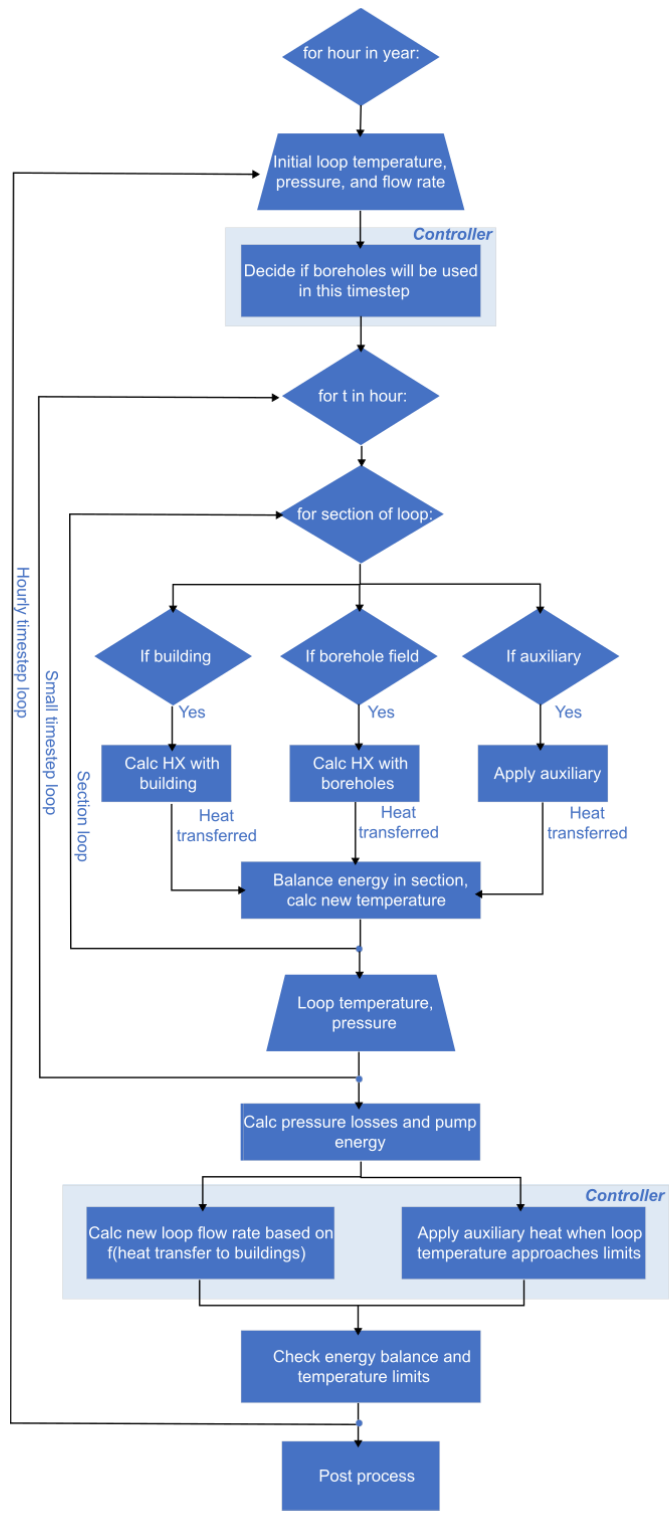

Figure 2. Reduced-order model process diagram

2.3 Controls

In Fig. 2, the three controller options are identified at the system level with light-blue boxes: borehole field, circulation pump, and auxiliary system. These are the three components in the model that are controllable on an hour-to-hour basis and represent what a utility can control on an as-built system. While these components could be controlled in many ways, the current methods used in the reduced-order model are described below.

The borehole controller acts as a bypass valve and decides if the thermal loop fluid will be pumped through the borehole fields in that hour or diverted around the borehole fields. The controller chooses to not use the borehole fields if the average thermal loop temperature is in the deadband—sufficiently far away from the designated thermal loop operating temperature bounds—for at least two consecutive hours. Otherwise, the thermal loop fluid is pumped through the borehole fields. This is a conservative approach that avoids quick cycling of the borehole fields and maintains a thermal loop temperature near the middle of its acceptable range, usually based on heat pump operation. The deadband within which the borehole fields are bypassed could be adjusted for different systems designs or operational goals.

The circulation pump flow rate controller adjusts the mass flow rate based on the total building thermal load in the last timestep. The goal is to run at the lowest speed possible (to minimize pump energy use and maximize heat transfer) while also avoiding large temperature changes from house to house along the thermal loop. A relationship between flow rate and building load was found from fully steady-state simulations (shown in Fig. 3) and is used in the semi-transient model here. In the steady-state simulations, the flow rate was iteratively adjusted at each timestep to find the minimum flow rate that maintained the thermal loop temperature within bounds and did not allow for excessive change in temperature between borehole fields. A simple piecewise function was fitted to the data to predict the best thermal loop flow rate given the total user load on the system. Note that identifying one constant thermal loop temperature to use for the whole year is not how a geothermal network would operate in a real-world application and is difficult (if not impossible, depending on the thermal loop configuration) because high flow rates are needed to avoid significant temperature changes on the thermal loop but high flow rates reduce the heat transfer with the borehole fields and thus may not be able to maintain a temperature within the specified system bounds.

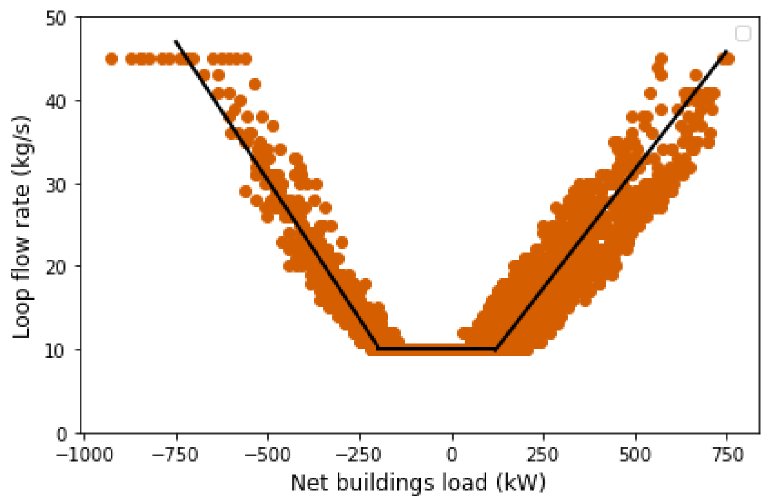

Figure 3. Steady-state simulation results with fitted piecewise curve to predict necessary thermal loop flow rate based on net building load (into the thermal loop) for the whole district.

The auxiliary heating and cooling system is used to track any additional energy needed to balance the system and thus does not have a complex end use model. If the minimum or maximum thermal loop temperature is within 3.5°C of the temperature bounds, then the auxiliary system adds or subtracts a heat rate in 100 kW intervals to or from the thermal loop, based on if the thermal loop needs additional heating or cooling, respectively. If the thermal loop temperature is not within 3.5°C of the temperature bounds, then the auxiliary heating or cooling is slowly removed, ramping up or down by 100 kW each timestep, until it reaches zero.

3. APPLICATION OF MODEL

The example system modeled here is an estimate of a geothermal network being installed in Framingham, MA. The location, ground temperature, and number of building loads are all representative of the Framingham installation. However, we do not attempt to match the exact details of the system, including the borehole field configuration, both due to a lack of data and to protect participating customer privacy. Therefore, the example design studied herein is *not* representative of any specific configuration or the views, plans, or designs of the Framingham, MA installation. The goal of this study is rather to demonstrate the capabilities of this proposed reduced-order model which will be used to simulate more specific geothermal networks in the future.

The geothermal network installation modeled in this study includes 37 buildings, mostly single-family homes with a mix of other building types including municipal and commercial buildings. The system considered herein uses a single pipe connecting all the buildings in the district in a thermal loop, known as a reservoir network (Sommer et al., 2020). Note that the time for the fluid to fully circle the thermal loop will vary based on the size of the loop and the speed of the fluid. For this example system, the thermal loop is approximately 1600 m long and the fluid takes about an hour on average to fully circulate the loop. The upper and lower operational temperature limits are 35°C and 0°C, respectively, for all components in the geothermal network, and the working fluid in the loop is 25% propylene glycol. The borehole controller deadband where the borehole fields are bypassed is 12-23°C.

For this simulation, the thermal loop was divided into 30 sections, each with a length of 54 m and a fluid mass of 1792 kg. The use of 30 sections was found to give similar results to a 50-section simulation (where nearly every loop element is in its own section) while requiring only a fraction of the computational time. The elements found in each section of the thermal loop are listed in Table A1 in the Appendix. Note that some sections have no elements due to the physical location of different users around the thermal loop. As it is a loop, the fluid leaving section 29 at a given timestep will enter section 0 at the next timestep.

4. RESULTS AND DISCUSSION

The reduced-order model is used to simulate one year of operation for the given example system to establish a baseline of outcomes. Then, the effect of different control strategies is investigated. The model is run with and without the borehole controller and the effects on the system are shown and potential tradeoffs are discussed.

4.1 Example system performance

Example results from simulating the given system configuration are shown in Figs. 4-6, with the auxiliary system, circulation pump, and borehole field controllers all operating as described in Section 2.3.

Figure 4 compares section temperatures (for each of the 30 sections the loop is subdivided into for modeling) throughout the thermal loop at one timestep in the summer (June) and one timestep in the winter (December), plotting T_1. The sections that include borehole fields are noted. The temperature in the thermal loop can be seen to generally rise in the summer and fall in the winter as the working fluid moves around the thermal loop and then return closer to the ground temperature (12°C) when passing through a borehole field. The thermal loop flow rate is minimized while still preventing significant changes in temperature between borehole fields. While these results are not surprising, Fig. 4 confirms that the thermal loop model is operating as expected and demonstrates that detailed information can be output about the spatial distribution of the working fluid temperature around the loop.

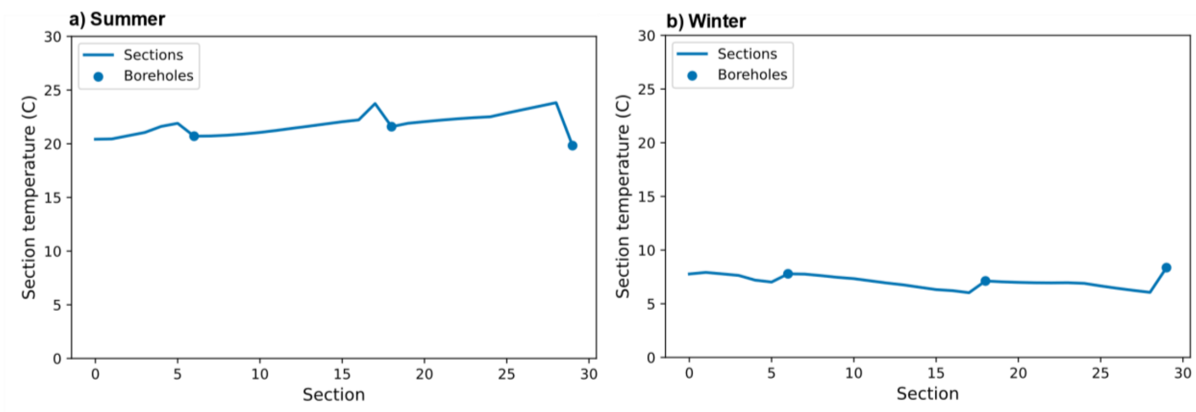

Figure 4. Section temperatures of the thermal loop in a) summer and b) winter, where the sections that include boreholes are shown with points.

The thermal loop average temperature (across all sections) and flow rate for each hour of the year is shown in Fig. 5.

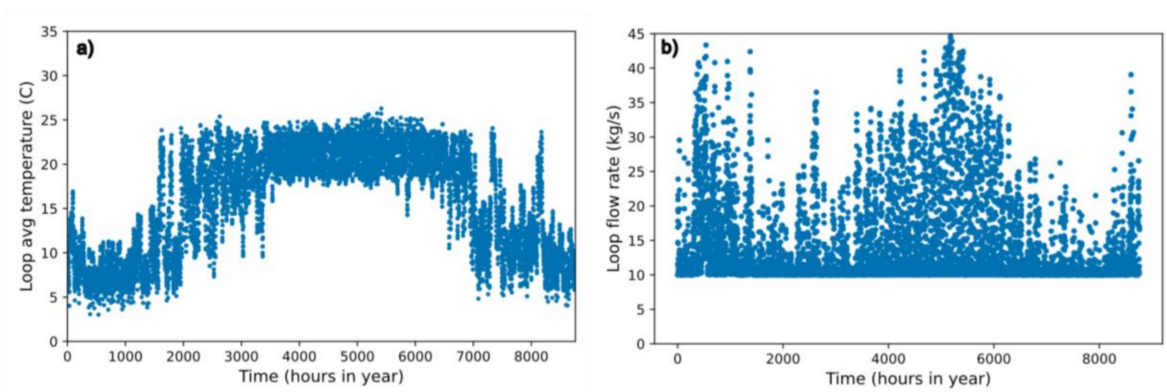

Figure 5. a) average temperature, b) flow rate of the thermal loop for each hour of the year.

The thermal loop temperature is always maintained between the imposed temperature bounds of 0°C and 35°C. The temperature is roughly centered around the temperature of the boreholes (which start at 12°C), but the thermal loop temperature is allowed to vary up or down throughout the year. The thermal loop flow rate is set based on a relationship with total building load (Fig. 3). The loop flow rates are highest in the winter and summer—when heating and cooling loads are highest.

The total heat rate into the thermal loop is plotted over the year in Fig. 6 for building loads, borehole fields heat transfer, and auxiliary system input. The borehole fields modeled herein are able to balance the building load most of the year, but the auxiliary system provides some additional heat in the winter. Note that the actual installation in Framingham, MA has borehole fields designed to need no auxiliary heat.

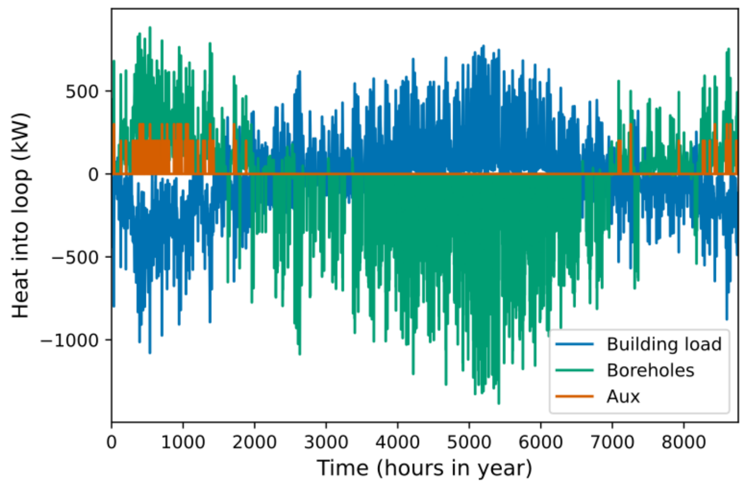

Figure 6. Heat rate into the thermal loop over a year, where positive denotes heat in and negative denotes heat out. Heat is exchanged with buildings, borehole fields, and the auxiliary system (Aux).

Though the economic portion of this model is still being developed, additional potential outputs from the model include total electricity usage, expected electrical bills for users, and LCOH of the system.

4.2 Control impact

Once the baseline performance of the model was assessed and the model capabilities plotted using all control strategies from Section 2.3, the impact of removing controllers was considered. When the auxiliary system controller or circulation pump controller are removed, the system fails to stay within the specified operational bounds. This may result in freezing of the working fluid in the thermal loop or failure to meet user loads. Thus, we will instead compare results with and without the borehole controller because both cases are able to stay within the set bounds while still showing distinct differences.

Without the borehole controller regulating the use of the boreholes, the default is to use the boreholes continuously and the pumps are never turned off. With the borehole controller applied to the given example system, the boreholes are valved off and the pumps do not run when the thermal loop average temperature is in the dead band (between 12-23°C) for at least two consecutive hours.

Comparing the cases with and without the borehole controller, the system average flow rate, auxiliary heating input, and peak total electricity did not change. Thus, the general performance of the system was not greatly affected; the changes due to the borehole field operation were confined primarily to temperature changes and electricity usage. The simulation results of selected variables that did exhibit differences are shown in Table 1: average thermal loop temperature, total electricity usage from all components over a year, annual example single-family home electricity usage, annual example commercial building electricity usage, and total electricity usage from the borehole fields.

Table 1. Annual simulation results with and without borehole controller

	Avg loop temp (°C)	Total elec (MWh)	Single-family home elec (MWh)	Commercial building elec (MWh)	Total borehole field elec (MWh)
Constant borehole operation	12.7	383	2.38	7.44	52.23
Borehole controller	15.8	374	2.39	7.76	34.83
Percent change from implementing controller	25%	-2%	0%	4%	-33%

Implementing a controller that turns off the boreholes when the thermal loop temperature is moderate results in a large reduction in electricity consumption from the borehole field pumps and a slight reduction (2%) in the total system electricity consumption. Additionally, the average thermal loop temperature is slightly higher.

The energy usage for the heat pump in a single representative single family and single commercial building are also shown. For individual buildings, there are only small electricity use impacts compared to the total system electrical usage but these represent the load that users would be directly responsible for and would see on their electrical bill. Thus, changes to the building electrical loads should also be monitored as they have direct user impact and understanding this impact will inform fair ratemaking practices for utility customers served by the network.

Overall, the total annual electricity consumption is reduced by using a borehole controller, but the effect is not uniform across the system. The increased thermal loop temperature, particularly in the summertime, results in a slight decrease in heat pump COP for cooling and a slight increase in user annual electrical bills. For a residential consumer with low cooling demand, the change is negligible, but for a commercial customer with higher cooling demand, the change is more noticeable. In Table 1 the commercial building is estimated to have a 4% increase in annual electricity load to meet its demand. The system operator would need to balance this trade-off between reducing operational power consumption and increasing user power consumption.

5. CONCLUSIONS AND FUTURE WORK

We developed a reduced-order model for simulating a single-pipe ambient-temperature loop 5G DES and applied it to a geothermal network that connects ground-source heat pumps in commercial and residential buildings to manage their thermal load. For now, this study outlines the methodology of the reduced-order model and then shows results for an example system. The potential benefits of the reduced-order model include being able to track heat flows in the system, substitute simple or complex models for each component, as needed, and monitor electricity usage from all components. Simple controllers have been developed for the borehole fields, circulation pump, and auxiliary heating and cooling system. While the reduced-order model makes many simplifying assumptions for fast computation, it is still able to capture the flow of heat and the effect of thermal inertia in the thermal loop.

The impact of using a bypass controller for the borehole fields versus running them continuously is demonstrated with an example case. Using the controller significantly reduces the power consumption of the borehole field pumps and slightly reduces the electricity consumption of the system overall in the example case. However, using the borehole controller also increases the electrical consumption for the users due to higher thermal loop temperatures in the summertime months when cooling is needed. These tradeoffs may be minimized through other loop control or design choices and should be investigated further when determining how to operate and regulate a geothermal network.

Next steps for this model include simulating an actual installation and validating it against operational data. This model will be validated in the future against data from multiple utility-led geothermal network installations in Massachusetts. Once validated, further research into optimization of the system and the tradeoffs between optimal performance of different components can be considered. Additionally, this model could be used to analyze whether a geothermal network would result in even more substantial benefits to the electrical grid as compared to geothermal heat pumps on individual buildings.

ACKNOWLEDGEMENTS

This work was authored by the National Renewable Energy Laboratory, operated by Alliance for Sustainable Energy, LLC, for the U.S. Department of Energy (DOE) under Contract No. DE-AC36-08GO28308. Support for the work was provided by the Home Energy Efficiency Team (HEET) under FIA-22-23124, supported by a grant from the Massachusetts Clean Energy Center (MassCEC) to HEET entitled: Learning from the Ground Up (LeGUp). The views expressed herein do not necessarily represent the views of the DOE, the U.S. Government, or MassCEC.

The authors would like to acknowledge the contributions of Isabel Varela, Eric Juma, Angie Alberto Escobar, Zeyneb Magavi, and others at HEET as well as Jianjun Hu, Christine Doughty, and Yingqi Zhang at Lawrence Berkeley National Lab (LBNL). A particular thanks to Jianjun Hu for running the simulations to create the borehole field lookup tables.

REFERENCES

Bergman, T. L., Lavine, A. S., Incropera, F. P., & Dewitt, D. P. (2011). *Fundamentals of Heat and Mass Transfer*. Wiley.

Buffa, S., Cozzini, M., D'Antoni, M., Baratieri, M., & Fedrizzi, R. (2019). 5th generation district heating and cooling systems: A review of existing cases in Europe. *Renewable and Sustainable Energy Reviews*, *104*, 504–522. https://doi.org/10.1016/j.rser.2018.12.059

Climatemaster. (2022). *Tranquility® 30 Digital (TE) Series Submittal Data*. https://files.climatemaster.com/lc991-climatemaster-commercial-tranquility-30-digital-two-stage-te-series-water-source-heat-pump-submittal-set.pdf

del Hoyo Arce, I., Herrero López, S., López Perez, S., Rämä, M., Klobut, K., & Febres, J. A. (2018). Models for fast modelling of district heating and cooling networks. *Renewable and Sustainable Energy Reviews*, *82*, 1863–1873. https://doi.org/10.1016/j.rser.2017.06.109

EPRI. (2021, February). Efficiency Electrification. *Electric Power Research Institute*. https://publicdownload.epri.com/PublicAttachmentDownload.svc/AttachmentId=70746

Kontar, R. E., Polly, B., Charan, T., Fleming, K., Moore, N., Long, N., & Goldwasser, D. (2020). *URBANopt: An Open-Source Software Development Kit for Community and Urban District Energy Modeling: Preprint*.

Lawrence Berkeley National Laboratory. (n.d.). *Modelica Buildings Library* [Computer software]. https://simulationresearch.lbl.gov/modelica/

Liu, X., Ho, J., Lian, J., Wang, X., Liu, W., Malhotra, M., Li, Y., Prem Anand Jayaprabha, J. A., & Li, F. (2023). *Grid Cost and Total Emissions Reductions Through Mass Deployment of Geothermal Heat Pumps for Building Heating and Cooling Electrification in the United States* (ORNL/TM-2023/2966, 2224191; p. ORNL/TM-2023/2966, 2224191). https://doi.org/10.2172/2224191

Marin, C. (2022, February 3). Austin's Whisper Valley GeoGrid™ Proves to be Resilient Sustainable Energy Solution After Extreme Weather and Grid Events. *Business Wire*. https://www.businesswire.com/news/home/20220203005848/en/Austin%E2%80%99s-Whisper-Valley-GeoGrid%E2%84%A2-Proves-to-be-Resilient-Sustainable-Energy-Solution-After-Extreme-Weather-and-Grid-Events

Mitchell, M., & Lee, E. (2022). *SecondaryCoolantProps* (1.1) [Python]. https://secondarycoolantprops.readthedocs.io/en/latest/

Oh, H., & Beckers, K. (2023). Cost and Performance Analysis for Five Existing Geothermal Heat Pump-Based District Energy Systems in the United States. *Renewable Energy*.

Quirosa, G., Torres, M., & Chacartegui, R. (2022). Analysis of the integration of photovoltaic excess into a 5th generation district heating and cooling system for network energy storage. *Energy*, *239*. https://doi.org/10.1016/j.energy.2021.122202

Sommer, T., Sulzer, M., Wetter, M., Sotnikov, A., Mennel, S., & Stettler, C. (2020). The reservoir network: A new network topology for district heating and cooling. *Energy*, *199*, 117418. https://doi.org/10.1016/j.energy.2020.117418

Wolfson, G., & Mapel, M. (2020, September 29). *The Importance of Nanogrids in Low-Carbon Residential Communities*. Whisper Valley. https://www.whispervalleyaustin.com/the-importance-of-nanogrids-in-low-carbon-residential-communities/

Xcel Energy. (2023). *Evaluating a community ground source heat pump system at Colorado Mesa University*.

Zarin Pass, R., Wetter, M., & Piette, M. A. (2018). A thermodynamic analysis of a novel bidirectional district heating and cooling network. *Energy*, *144*, 20–30. https://doi.org/10.1016/j.energy.2017.11.122

APPENDIX

Table A1. Elements in each section of the thermal loop

Section	Elements
0	Municipal building
1	-
2	Multi-family homes
3	Multi-family homes
4	Multi-family homes
5	Multi-family homes
6	Borehole field
7	1 Single family home
8	3 Single family homes
9	3 Single family homes
10	2 Single family homes
11	3 Single family homes
12	3 Single family homes
13	2 Single family homes
14	3 Single family homes
15	3 Single family homes
16	-
17	Commercial building
18	Borehole field, municipal building
19	Commercial building
20	-
21	-
22	-
23	-
24	Municipal building
25	Multi-family homes
26	Multi-family homes
27	Multi-family homes
28	Multi-family homes
29	Borehole field, circulation pump, auxiliary